Journal of Materials Chemistry A

ROYAL SOCIETY OF CHEMISTRY

PAPER

View Article Online
View Journal | View Issue

Cite this: J. Mater. Chem. A, 2025, 13, 31755

The impact of low-intensity illumination on the reverse bias behavior of perovskite solar cells

Jonathan Henzel, *[ab] Klaas Bakker, [a] Sjoerd Veenstra, [a] Olindo Isabella, [b] Luana Mazzarella, [b] Arthur Weeber [b] and Mirjam Theelen [a]

Received 21st May 2025
Accepted 31st July 2025

DOI: 10.1039/d5ta04100g

rsc.li/materials-a

In realistic partial shading scenarios, the impact of low-intensity illumination needs to be considered. However, there is barely any research available and the published results are contradictory. Here, it is shown that the reverse bias behavior of perovskite solar cells under low-intensity illumination strongly depends on the voltage scan rate. As explanation, a hypothesis is developed and experimentally verified that is based on two antagonistic mechanisms: on one hand, illumination affects the mobile ions conductivity, decreasing the breakdown voltage. On the other hand, an electrochemical reaction caused by the reverse bias current increases the breakdown voltage. Since the two mechanisms occur on slightly different time scales, it depends on the voltage scan rate which mechanism dominates. These findings emphasize that more detailed research into the mechanism occurring in reverse bias and the factors affecting the reverse bias breakdown is still necessary. Firstly, a deeper understanding would be helpful for investigating the effect of realistic, non-ideal partial shading scenarios on perovskite modules. Secondly, knowing how cell properties and external factors influence the breakdown voltage is necessary for defining standardized measurement procedures that allow the comparison of different perovskite solar cells in regards to their reverse bias stability.

1 Introduction

The power conversion efficiencies (PCEs) of perovskite solar cells (PSCs) are leaping from record to record. With small-area cells having reached nearly 27%, and even perovskite mini-modules with 23.2% being revealed,[1] it seems that the commercial breakthrough is only a question of time.

However, there are still some hurdles that need to be overcome first. One important challenge is the stability. Just like with the efficiency, the bar is set by the dominating silicon (Si) PV technology where panels generally come with a warranty of 25–30 years, guaranteeing that during this time, degradation remains below 0.4–0.6% per year.[2] That is a significantly longer period of time than the age of the perovskite in PV technologies in general (use in dye-sensitized solar cells since 2009).[3] One of the longest reported outdoor tests of perovskite solar cells until now lasted only around 2.5 years.[4]

Accelerated lifetime testing is required, where unrealistically harsh conditions are used to imitate the effects of long-term outdoor exposure. Here, challenges lie in only accelerating those degradation pathways relevant to outdoor exposure and in the need to translate the results of indoor tests into predictions of outdoor lifetime of modules. While these challenges pose questions yet to be answered in full, there exists a framework of defined testing conditions whose purpose it is to improve the comparability of stability experiments on (among other technologies) perovskite solar cells:[5] the authors of the ISOS protocols (International Summit on Organic Photovoltaic Stability) name various stressors that can be expected to occur under operating conditions and cause changes in perovskite solar cells.[5] One such stressor is the occurrence of reverse biases (RB).

Reverse biases are an especially serious problem in monolithically interconnected modules which is the preferred module design for thin-film PV technologies. There, a module consists of thin, but long, stripe-like cells which are electrically-connected in series. That means that one and the same current is flowing through all cells. This monolithic interconnection provides advantages but leads to problems when current is not generated homogeneously across the module area. This can occur, for instance, due to disparate aging or partial shading.[6]

During a typically considered partial shading event, a part of a module, *e.g.* one cell, is completely shaded. This scenario has been named 'asymmetric' partial shading by Dongaonkar *et al.*[7] There, all cells but one are fully illuminated while the one shaded cell operates in darkness and does not generate any current. Since the shaded cell is series-connected to the illuminated cells, the shaded cell has to pass the current generated by them. That leads to the accumulation of charge carriers at the interfaces and the build-up of an electric field. This electric

[a]TNO, High Tech Campus 21, 5656 AE Eindhoven, Netherlands. E-mail: jonathan.henzel@tno.nl
[b]Delft University of Technology, Mekelweg 4, 2628 CD Delft, Netherlands

field is oriented in the opposite direction to the electric fields in the illuminated cells. Therefore, the voltage dropping over the shaded cell is negative. This voltage is called 'reverse bias'.

This reverse bias grows, until either the shaded cell passes the current generated by the other cells, or the maximum voltage that the illuminated cells can generate is reached. This maximum reverse bias is the sum of the open-circuit voltages (V_{oc}) of the illuminated cells. In this case, no current flows through the cells of that module and no power can be extracted. In the other, more realistic case, however, the shaded cell breaks down, the current is passed and the module continues to generate power at the price of the shaded cell operating in reverse bias.

There are several publications available that investigate the effect of partial shading on perovskite modules: a detailed discussion of the effects of partial shading and possible methods of mitigation (bypass diodes, module design, cell geometries), including their problems, can be found in Wolf *et al.*[8] Experimental results of partial shading experiments on perovskite (mini-)modules have been presented by Bogachuk *et al.*, Yang *et al.*, Tayagaki *et al.*, and Aninat *et al.*[9–12] Additionally, inspiration can be found in the research that has already been performed on other thin-film PV technologies: when it comes to module design or interconnection strategies, or considerations of realistic partial shading scenarios, lessons from research on CIGS modules can come handy.[7,13,14]

Nonetheless, the impact of reverse bias on a single solar cell was the focus of most publications at present. Instead of investigating the effects of a partial shading event on a perovskite module, a reverse bias is directly applied to a single perovskite solar cell in the dark. This allows the investigation of the effects of reverse biases without being hindered by the problems of fabricating modules with enough cells to force a shaded cell into breakdown while maintaining a device quality that is relevant for degradation experiments. This method of applying reverse biases to single cells has been successful in demonstrating the devastating impact that this degradation mode has on perovskite solar cells and in investigating the degradation pathways that serve to quickly decrease the PCE. The phenomenological works of Razera *et al.*[15] and of Bowring *et al.*[16] form the basis of all research in this field. A more general overview can be found in Wang *et al.*[17]

An important point is that it seems that degradation is driven by the reverse bias current and not by the reverse bias itself.[18,19] It follows that the reverse bias breakdown (V_{BD}) has to be avoided in order to limit the reverse bias current and therefore retard degradation. In modules, that necessitates the use of bypass diodes that provide low-resistance current paths above a certain voltage threshold. One question is how to integrate bypass-diodes into the modules: the problems related to this question are illustrated and discussed in Bowring *et al.*[16] and Wolf *et al.*[8] Another hurdle to overcome is the cost effectiveness which is directly related to the number of bypass diodes required. The number of bypass diodes is, in turn, related to the breakdown voltage of the perovskite solar cells that are to be protected.[8] A larger (*i.e.* a "more negative") breakdown voltage reduces the number of bypass diodes needed.

Accordingly, significant effort has been focused on manipulating the breakdown voltage towards larger values by introducing additives or additional layers to the perovskite solar cell layer stack.[20–25]

An important aspect that has only very recently received attention is the interaction between reverse biases and illumination. At the first glance, adding illumination to a phenomenon that occurs during a partial shading event (as defined above) might seem less relevant. There are, however, two scenarios during which the impact of illumination might be important:

(1) Perfect shading, that is, complete darkness in the shaded area, is probably quite rare in real operating conditions. Whenever the object that is casting the shadow is located at a distance from the module, some diffuse illumination will still reach the 'shaded' module area. Additionally, when considering the trend towards bifaciality, even perfect shading from one side might not prevent diffuse illumination from the other side.

(2) Partial shading might not follow a simple pattern as posited for the simplified asymmetric shading case where one or more cells of a module are completely shaded.[7] A more realistic scenario expects the 'realistic' shading case (named by Dongaonkar *et al.*) where only a part of a cell area is shaded while the remaining area is illuminated.[7] This illumination can be of low-intensity as in the first scenario.

In CIGS solar cells, it was shown that illumination causes a significant reduction of the breakdown voltage.[26,27] This effect would mean for the first scenario of incomplete but spatially-homogeneous shading that the effective V_{BD} would be lower than measurements in the dark show. This would have implications for the number of bypass-diodes required. Following the second scenario of incomplete and inhomogeneous shading, local, low-intensity illumination would lead to a locally lower V_{BD}. If a part of a cell that operates in reverse bias has a lower V_{BD}, we expect most of the reverse bias current to flow there. This locally concentrated reverse bias current would lead to locally increased degradation. Aninat *et al.* recently proposed this explanation for locally increased partial shading degradation observed in a perovskite module.[12]

Nevertheless, there have been only few publications that mention the interaction of reverse bias with illumination in PSCs: Jiang *et al.* observed that an illumination intensity of 0.1 suns did only have a negligible effect on the breakdown voltage.[25] Wang *et al.*, on the other hand, found that the breakdown voltage changes drastically upon adding low-intensity illumination.[28] They considered an illumination wavelength-dependent mechanism as in CIGS but also emphasized the possible importance of mobile defects.[28]

In all these publications, the topic of reverse bias under illumination has only been treated peripherally. That means that a detailed investigation with a proposed mechanism is still missing. The qualitatively different observations regarding the impact of illumination on the breakdown voltage in the presented literature serve as proof that there is a phenomenon worth investigating. Together with the possibly great relevance of this topic for the partial shading stability of PSCs, this

discrepancy serves as motivation for us to take a more detailed look at the interaction of reverse biases with illumination.

In this publication, we present an investigation of this interaction between reverse bias and illumination. We varied various experimental parameters (scan rate, illumination intensity, illumination wavelength) and built up on our results by developing a mechanism to explain the observed phenomena. Finally, we designed and executed experiments to test our hypothesis.

2 The effects of illumination on the reverse bias behavior in voltage sweeps

2.1 The voltage sweep experiment

Our samples are p–i–n structured, semi-transparent perovskite solar cells with a triple-cation (Cs, Ma, FA), double-halide (Br, I) absorber composition. The layer stack consists of glass/ITO/PTAA/PVK/C_{60}/SnO_2/ITO. Details about fabrication and the results of the initial characterization in the SI; the latter in SI Fig. 1 to 3. The detailed measurement parameters used throughout this publication if not mentioned differently are available there as well.

There are three parameters whose impact on the breakdown voltage we want to investigate: the illumination intensity, the wavelength of the illumination, and the voltage scan rate. While the former two parameters also play a role in the mechanism described for CIGS,[26] varying the scan rate reveals the impact of mobile ions and other slow processes unique to PSCs.[29]

To that end, we executed an experimental procedure that is schematically depicted in Fig. 1. This experiment consisted of reverse bias (RB-)*JV* measurements with a voltage range that is extended into the reverse bias regime. We always performed both a reverse (RV) sweep (from 1 V to −8 V or to the current cutoff at −20 mA cm^{-2}) and a forward (FW) sweep (from −8 V or the current cutoff to 1 V). These RB-*JV* measurements were executed using five different voltage scan rates (between 5 V s^{-1} and 0.1 V s^{-1}). For every voltage scan rate, we performed eight dark RB-*JV* measurements and seven light RB-*JV* measurements (Fig. 1a). We call such a set of 15 RB-*JV* measurements a "group".

The dark and light RB-*JV* measurements were alternated in order to use the latest dark measurement as baseline for the following light measurement (see Fig. 1b and c). That way, we were able to correct for changes to the cell due to previous measurements. A set of a dark and corresponding light RB-*JV* measurement is called a "pair".

The illumination intensity (expressed as a ratio $P_{light} = J_{sc}^{light}/J_{sc}^{1sun}$) was successively increased from light measurement to light measurement. As light source, we used a blue (455 nm), green (530 nm) or far red (735 nm) LED. The purpose of using different wavelengths were the resulting different absorption profiles which might reveal information about the role of the interfaces between the absorber and the transport layers.

Fig. 1d shows how we analyzed the data: we corrected for the photo-generated current by subtracting J_{sc}: $J_{RB} = J - J_{sc}$. the breakdown voltage V_{BD} is defined using a fixed current density: $V_{BD} = V@ - 10$ mA cm^{-2}. In general, we will describe the absolute value of the breakdown voltage. Therefore, a "larger V_{BD}" means a more negative breakdown voltage. The difference between the V_{BD} under illumination and the V_{BD} in the dark is defined as the breakdown voltage shift ΔV_{BD}.

2.2 Initial results

Fig. 2 shows representative results from this experiment, using a blue LED as light source. Only the RV sweeps are displayed. The FW sweeps and results from other cells can be found in the SI (Fig. 4–6). The general observations match.

Fig. 2a displays the measurement results of a group of RB-*JV* measurements, using the voltage scan rate 5 V s^{-1}. The curves are corrected for the photo-generated current as described previously. The eight RB-*JV* measurements in the dark ("dark" RB-*JV*) are displayed as black curves and the seven RB-*JV* curves under illumination ("light" RB-*JV*) in various shades of red. The lightness of the color corresponds to the illumination intensity P_{light}, so that the darkest red curve belongs to the light RB-*JV* measurement with the smallest P_{light}. The horizontal, dashed line marks the current density selected to define V_{BD}.

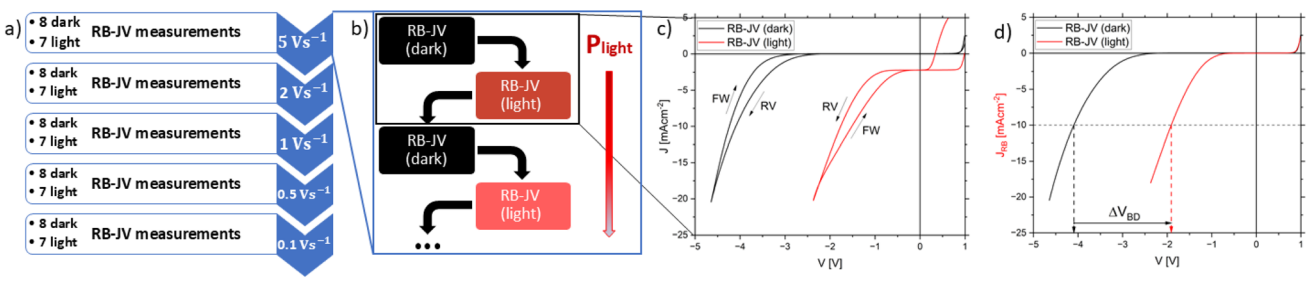

Fig. 1 The experimental procedure and analysis: (a) shows the five groups of reverse bias (RB-) *JV* measurements that each consist of eight dark and seven light RB-*JV* measurements. Within each group of measurements, one voltage scan rate was used. We started with the group with the highest scan rate and proceeded towards the smaller scan rates. (b) Shows the first four RB-*JV* measurements of a group. Dark and light RB-*JV* measurements were alternated and the illumination intensity P_{light} was increased light RB-*JV*-to-light RB-*JV*. (c) Shows one such pair of one dark (black) and one light (red) RB-*JV* measurement. Each pair consists of a reverse (RV) sweep and a forward (FW) sweep. (d) Demonstrates how we have analyzed the measured data. It shows the RV sweeps of a pair of RB-*JV* measurements after the correction for the photo-generated current. The current density marked by a horizontal, dashed line is used for defining a V_{BD} for the dark and one for the light RB-*JV* curve. The difference between the two V_{BD}'s is the breakdown voltage shift ΔV_{BD}.

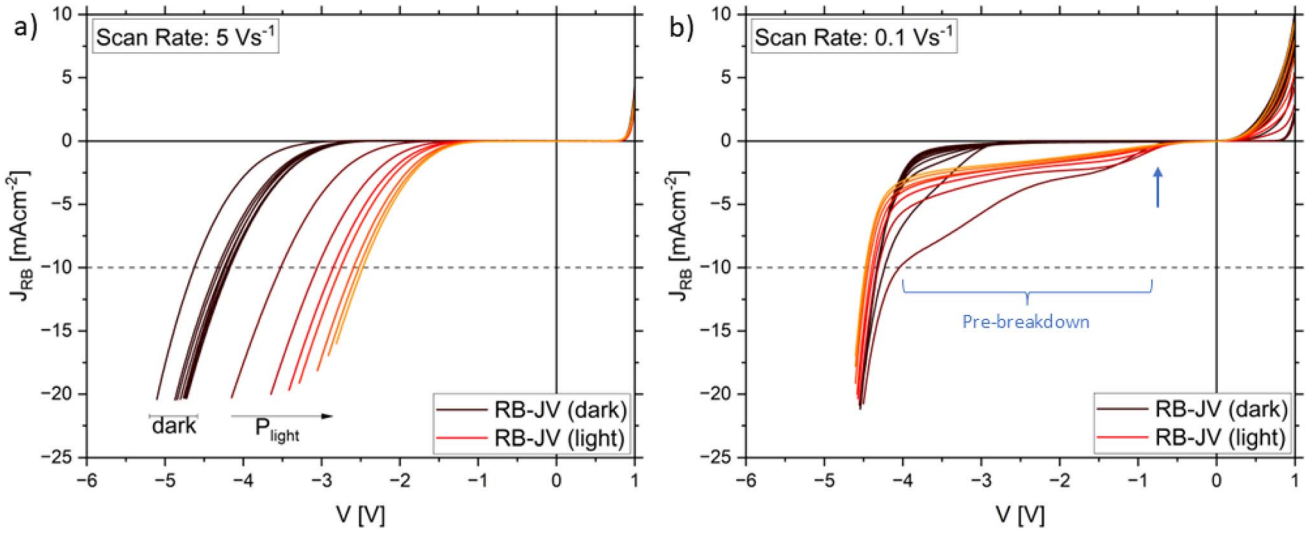

Fig. 2 Representative results of the experiment using a blue LED. (a) Shows the $J_{RB} = J - J_{sc}$ of the reverse (RV) sweeps with a scan rate of 5 V s^{-1}. The dark *JV* curves are shown in black, the light *JV* curves in various shades of red. The lightness of the color corresponds to the illumination intensity. A dashed, horizontal line marks the current density used for defining V_{BD}. (b) Shows the results for a scan rate of 0.1 V s^{-1} in the same way. There, a blue arrow marks the aborted early breakdown and a blue bracket the pre-breakdown of the RB-*JV* measurements under illumination.

Looking at the black curves, we see that most of them are nearly lying on top of each other. That means that also V_{BD} is nearly constant among them. Only one curve, corresponding to the first measurement, lies separate. Even then, however, the spread is smaller than 0.5 V (see, SI Fig. 7).

Contrary to the dark RB-*JV* curves, the light RB-*JV* curves (in red) do not lie on top of each other. Instead, we observe that they shift towards smaller voltages with increasing P_{light} (dark red to orange). Therefore, the V_{BD}'s under illumination move to smaller voltages. The difference between dark and light RB-*JV* curves grows and therefore ΔV_{BD} increases.

In Fig. 2b, another group of RB-*JV* measurements from the same experiment is displayed. Here, the scan rate was 0.1 V s^{-1}. Again, the black curves are the results from measurements in the dark while the red curves correspond to the measurements with increasing illumination intensity.

Looking at the dark RB-*JV* measurements first, we see that the black curves mostly overlap, again. One curve (corresponding to the first measurement) lies partially separate from the others. However, near the horizontal, dashed line, all black curves are close to each other, so that the spread of V_{BD} is small.

If we turn our attention to the light RB-*JV* curves (in red), we observe that the (absolute) current density begins to increase at a very small voltage ($V \approx -1$ V, marked by blue arrow). With increasing reverse bias, the current density proceeds to increase only slowly, however. This is a new phenomenon that we call 'pre-breakdown' (blue bracket). At a voltage $V \approx -4$ V, the current density suddenly increases steeply. Here, the actual breakdown occurs. This happens for all light RB-*JV* curves at nearly the same voltage. This means that V_{BD} is nearly the same for all light RB-*JV* measurements with this scan rate. As the difference between the dark and light RB-*JV* curves at −10 mA cm^{-2} is minimal, ΔV_{BD} is small.

We now proceed to comparing Fig. 2a and b, *i.e.* the results from measuring with 5 V s^{-1} and 0.1 V s^{-1}: when looking at the dark RB-*JV* curves first, we see a rather similar behavior. In both cases, the spread of V_{BD} is small, with the first measurement as outlier. Also, the V_{BD} of both groups lie around $V \approx -4.5$ V and not much more than 0.5 V apart from each other (see SI Fig. 7). We conclude that the scan rate (within the selected range) has only a limited impact on V_{BD} in the dark.

Comparing the light RB-*JV* curves shows significant differences: at 5 V s^{-1} (a), the light RB-*JV* curves and their V_{BD}'s shift significantly with P_{light}. In contrast, at 0.1 V s^{-1} (b), the V_{BD} is nearly unaffected by illumination. An additional difference is visible in the low current density regime ($J_{RB} \leq -3$ mA cm^{-2}): at 5 V s^{-1} (a), the light RB-*JV* curves look like dark RB-*JV* curves that have been shifted to smaller voltages. In contrast, the light RB-*JV* curves at 0.1 V s^{-1} (b) show the pre-breakdown and therefore completely different behavior than the corresponding dark RB-*JV* curves.

Finally, we take a look at the positive voltage region: in Fig. 2a, all the dark and light RB-*JV* curves lie on top of each other. It seems that neither the successive measurements nor the illumination has a lasting impact on the behavior in the positive voltage region. That is different at 0.1 V s^{-1} in Fig. 2b: there, we observe for both the dark and the light RB-*JV* curves, that the current density begins to increase at smaller positive voltages with every RB-*JV* measurement. As these are the RV sweeps that start at 1 V, it seems that the solar cells do not return to their initial state in between the measurements.

The corresponding results obtained from the FW sweeps are attached to the SI (Fig. 4) as they show qualitatively the same behavior. Only at the smallest scan rate of 0.1 V s^{-1}, a significant difference can be observed: the 'pre-breakdown' is completely absent in the forward sweeps (see also Fig. 6).

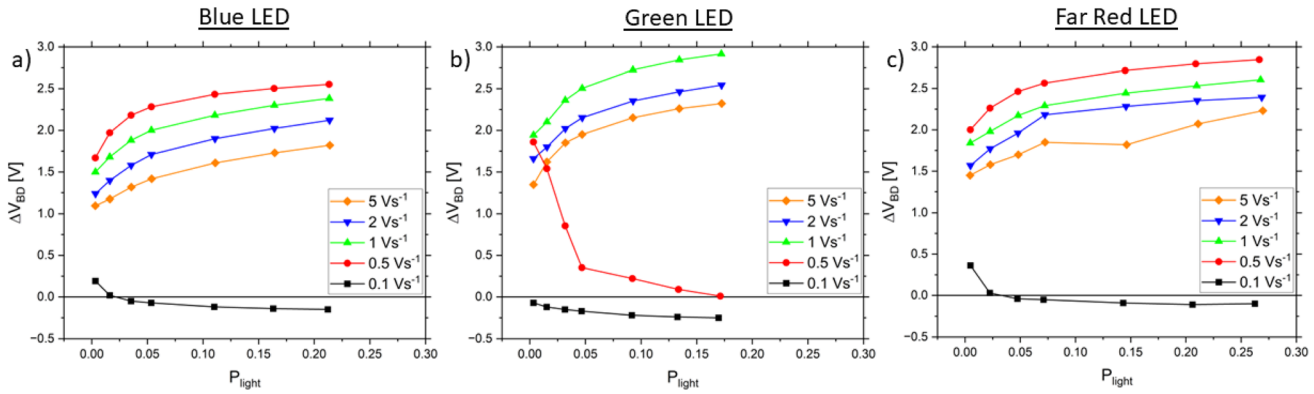

Fig. 3 Summary of the results of the experiments: the breakdown voltage shift (ΔV_{BD}), *i.e.* the difference in V_{BD} between the dark and the light RB-*JV* curves, is shown as function of the illumination intensity P_{light}. (a) Displays the results from blue illumination including the results shown in Fig. 2. (b) and (c) Show results from other cells for green and far red illumination, respectively.

The observations in regards to the V_{BD}'s are summarized for all investigated voltage scan rates and illumination wavelengths in Fig. 3 by means of comparing the breakdown voltages. To that end, the breakdown voltage shift (ΔV_{BD}), *i.e.* the difference between the V_{BD} in the dark and in the corresponding light RB-*JV* measurement, is plotted against the illumination intensity.

Fig. 3a shows results from the same cell as was shown in Fig. 2 on which blue illumination was used. We see two very different types of behavior: ΔV_{BD} is very small when using a scan rate of 0.1 V s^{-1} (black squares). In contrast, all other scan rates lead to ΔV_{BD}'s that range from 1 V to 2.5 V (orange, blue, green, and red symbols). These are the results from using scan rates $\geq$0.5 V s^{-1}. Additionally, a dependence on P_{light} is visible for these scan rates as well: at low illumination intensities, ΔV_{BD} increases steeply, but that increase levels off at $P_{light} \approx 0.05$. This might point to a logarithmic dependence (see semi-logarithmic plot in SI Fig. 8).

Fig. 3b and c show the results from experiments with different illumination wavelengths (green and far red) on other cells. It is clear that nearly the same behavior is observed as in Fig. 3a. The differences that are visible (especially in regards to 0.5 V s^{-1}, Fig. 3b) fall within the cell-to-cell variation and do not seem to be connected to the illumination wavelength (see the results from more cells in SI Fig. 6). We consider 0.5 V s^{-1} a boundary case where it varies from cell-to-cell whether it resembles the "fast" or the "slow" voltage sweeps.

The fact that the observed phenomenon does not depend on the wavelength of the illumination means that it does not depend on the absorption depth. That leads us to the conclusion that the mechanism responsible for the impact of illumination can occur in the whole perovskite layer.

2.3 Comparison with literature and open questions

Summarizing our observations, we can classify our results in two groups: when using a small voltage scan rate (*e.g.* 0.1 V s^{-1}), we observe the 'pre-breakdown' phenomenon but barely any change to the breakdown voltage. Indeed, V_{BD} even seems to be slightly larger under illumination than in darkness. In contrast, the results when using a higher voltage scan rate ($\geq$1 V s^{-1}) do show a significant change of the breakdown voltage. Here, the breakdown seems to occur at a far smaller voltage under illumination than in darkness. The magnitude of that shift shows a clear dependence on the scan rate and the illumination intensity. The scan rate 0.5 V s^{-1} seems to lie in the middle between the two cases. Generally, we did not observe any qualitative impact of the wavelength of the illumination in either case.

These results do fit to the observations in literature described above: Jiang *et al.* used a voltage scan rate of 0.35 V s^{-1} for reverse bias measurements with illumination and did not observe a significant impact of illumination.[25] The closest scan rate we used are 0.1 V s^{-1} and 0.5 V s^{-1}. The former did never show a significant impact of illumination, while for the latter, the results varied from cell to cell. We explain this with possible variations in material parameters, like mobile ions concentration, caused by details of fabrication. The same argumentation holds for the results of Jiang *et al.* However, the lack of 'pre-breakdown' in their results is a more significant difference. Later, we will show that this difference could be the result of a pre-conditioning of the cells before the measurement.

Wang *et al.* presented a significant impact of illumination on V_{BD}. Therefore, our observations seem to confirm the results of Wang *et al.*, although a direct comparison is difficult due to differences in sample structure and experiment design.[17] So, while there is an overlap between our observations and results reported in literature, there remain open questions:

- Why does illumination greatly influence the breakdown voltage when using high voltage scan rates?
- How can we explain the dependence of this breakdown voltage shift on scan rate and illumination intensity?
- What causes the 'pre-breakdown' phenomenon and why is the effect of illumination absent or even inverted at small scan rates?

In the following section, we develop a hypothesis that is able to explain the observed phenomena.

3 A detailed explanation

3.1 Developing a hypothesis on the effect of light and scan rate

Before we start formulating our hypothesis, we will give a short introduction to the generally-accepted reverse bias breakdown mechanism in perovskite solar cells that was proposed by Bowring *et al.*:[16]

This model posits that the breakdown mechanism is based on tunneling facilitated by the accumulation of mobile ions at the interfaces. Already without an external voltage, the built-in field leads to ion migration towards the interfaces until the bulk of the absorber is screened and most of the voltage drops near the interfaces. When a reverse bias is applied, additional mobile ions begin moving towards the interfaces until the external field is also screened. This accumulation of charged species leads to additional band bending which reduces the width of the tunneling barrier, thus increasing the probability for a tunneling event.[16]

A very simplified schematic of this breakdown mechanism is displayed in Fig. 4a. There, a certain concentration of mobile ions (red-filled circles) is present in the absorber of a PSC in darkness. Upon the application of a reverse bias ($-V$) and with enough time (Δt), these mobile ions move towards an interface with a transport layer (TL1). When they reach it, a reverse bias current (J_{RB}) begins to flow (red arrow).

In the publication of Bowring *et al.*, several factors are mentioned that add to the complexity of this mechanism:[16] for one, perovskite absorbers are generally polycrystalline materials with grains separated by grain boundaries. It is well-known that grain boundaries form channels for ion migration.[30,31] Secondly, there might be additional energy states within the tunneling barrier, opening the door for a trap-assisted tunneling mechanism. Additional factors could be macroscopic defects that are practically unavoidable in large-scale layer deposition and the impact of the electrodes on the electric field.[16,32,33] It should also be mentioned that there are also publications that discuss a possible role of an avalanche breakdown mechanism in perovskite devices.[17,34]

Finally, it was reported that the breakdown voltage is not a static property but changes during the application of a reverse bias: the breakdown voltage changes in time due to the slow migration of mobile ions. Additionally, the reverse bias current might itself cause an electrochemical reaction enhancing the tunneling barrier.[16] An enhanced tunneling barrier leads to a lower probability for tunneling and thus a decrease of the reverse bias current.

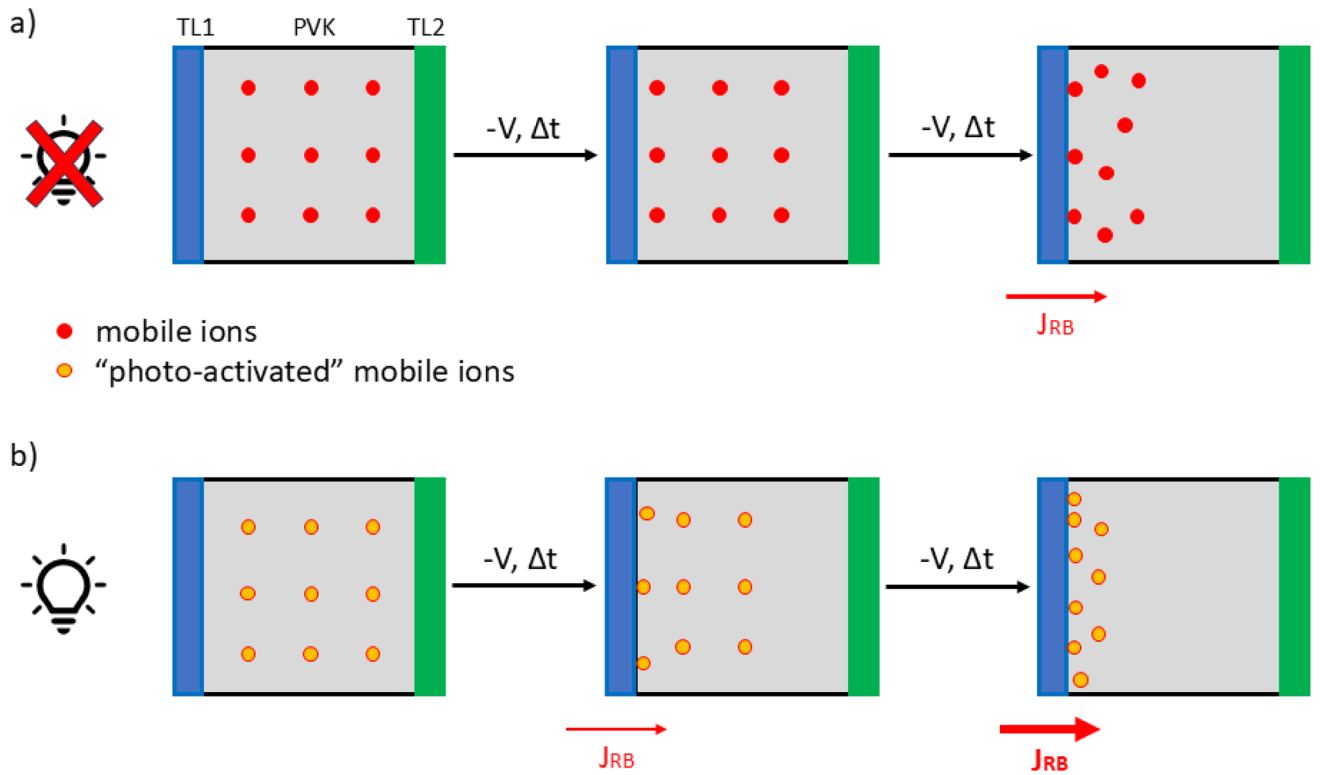

Fig. 4 A schematic representation of the reverse bias breakdown mechanism (a) in the dark and (b) under illumination. The effect of illumination is here presented as an increase of the mobility of the mobile ions by "photo-activation". A simplified schematic of a PSC with transport layers (TL1, TL2) and perovskite absorber (PVK) is depicted. The red-filled circles represent the mobile ions that are present in the dark while the orange-filled circles with red edge represent the photo-activated mobile ions with a higher mobility. When a reverse bias is applied ($-V$), both species move towards an interface which takes time (Δt). When they reach the interface, they contribute to the reverse bias breakdown mechanism and allow tunneling. That increases the reverse bias current (J_{RB}), depending on the number of mobile ions at the interface. Its magnitude is expressed as thickness of the red arrow.

To develop our hypothesis, we can draw inspiration from possibly related phenomena in PSCs: a phenomenon where the voltage scan rate has a significant impact on *JV* measurements under illumination is the *JV* hysteresis. There, the voltage sweep direction influences the results, *i.e.* the measured power conversion efficiency.[35] The general consensus on the origin of this hysteresis points toward the migration of mobile ion species and non-radiative recombination at interfaces.[36] Le Corre *et al.* demonstrated the impact of a wide range of voltage scan rates on the magnitude of hysteresis experimentally and connected their results to ion mobility by way of simulation.[29] They argued that a voltage scan at a very high scan rate (*e.g.* 1000 V s^{-1}) negates the impact of mobile ions as they cannot react to the changing bias. On the other hand, at very small scan rates (*e.g.* 0.01 V s^{-1}), the solar cell approaches steady-state as the mobile ions have enough time to reach a new equilibrium in between the measurement points.[29] In between these extrema, *JV* measurements show hysteresis. The scan rate where hysteresis reaches a peak in magnitude depends mostly on the diffusion coefficient of the mobile ions.[29] Their experiments were performed on solar cells considered to be "hysteresis-free" as they did not show significant hysteresis at a typical scan rates of about 0.1 V s^{-1}.[29] That matches our cells (see SI Fig. 1–3).

We can therefore assume that the impact of the scan rate must be connected to the ability of the mobile ions to react to the changing electric field during voltages sweeps. This ability depends on the mobility and concentration of the mobile ions and on how much time they have to reach a new equilibrium (Δt in Fig. 4a).

The impact of illumination on the mobile ions could come about indirectly *via* the temperature or directly. In the following, we will first investigate the possible effect of a temperature increase due to illumination.

Temperature could play a role since it has an effect on the mobile ions and on the reverse bias behavior. It has been reported in two publications that higher temperatures lead to smaller breakdown voltages.[11,16] This has been linked to quicker mobile ion movement.[16] As the voltage scan rate determines how long a cell is exposed to illumination, we could expect higher temperatures at smaller scan rates. This should lead to smaller V_{BD} values.

To get an idea about the temperature changes we can expect, we used an infrared (IR) camera to track the surface temperature of a PSC. After a few seconds without illumination, we switched on a blue LED, set to an intensity equivalent to $P_{light} = 0.25$. As this illumination intensity is among the upper limit of what we used during the voltage sweep experiments, this gives us also the upper limit of temperature increase. The detailed results can be found in the SI (Fig. 9). They show that even after 3 minutes of constant illumination (approximately the duration of a complete voltage sweep at 0.1 V s^{-1}), the temperature has only increased by about 3 K.

Therefore, the temperature cannot be expected to play a significant role, especially at smaller illumination intensities than $P_{light} = 0.25$. Since most of the ΔV_{BD} is, however, already visible at illumination intensities $P_{light} \leq 0.05$, another factor seems to be responsible for affecting the mobile ions.

The temperature could, however, be playing a role in the differences in ΔV_{BD} of the fast voltage sweeps ($\geq$0.5 V s^{-1}). There, we observe larger ΔV_{BD} values with smaller scan rates (see Fig. 3). That could be explained by higher temperatures due to longer scan durations. However, there is evidence against this temperature effect playing an important role here, as well: the difference between the ΔV_{BD} of the different scan rates stay constant for all illumination intensities. This observation argues against an impact of the temperature increase due to illumination. Therefore, we conclude that the illumination influences the mobile ions *via* a different mechanism than the temperature.

The impact of illumination on the mobile ions has been an object of research, based on the observation that the capacitance of solar cells at small frequencies increases significantly upon addition of illumination.[37] As origin of this observation, a reduction of the activation energy of mobile ions and the additional creation of defects were discussed.[38,39] However, conclusive answers even to fundamental questions regarding mobile ions species or mechanisms of ion migration or interaction with illumination are missing. Recently, Schiller *et al.* showed that the capacity-increase is caused by the photo-induced electronic currents being modulated by mobile ions and can therefore be explained without a change to ion mobility or ion concentration.[40] However, they still found evidence of a photo-conductive effect, meaning that illumination does indeed impact the ion conductivity. They did not specify whether it is the concentration or the mobility of the mobile ions that is affected by light. Developing a mechanism of interaction between light and ions was beyond the scope of their publication.[40] They did, however, argue that any interaction between illumination and mobile ions has to be mediated by photo-generated charge carriers.[40]

With that, we can incorporate the effect of illumination: light increases the conductivity of mobile ions, *i.e.* the concentration and/or mobility. These, in turn, affect the reverse bias behavior of perovskite solar cells. This is displayed in Fig. 4b. There, the effect of illumination is depicted as the photo-activation of mobile ions which increases their mobility. The mobility affects how fast the mobile ions move under a certain reverse bias ($-V$): due to the higher mobility under illumination, the photo-activated mobile ions reach the interface earlier than in darkness. More ions at the interface leads to stronger band bending and therefore a higher tunneling current. Thus, J_{RB} is larger under illumination. This is shown in Fig. 4b as a thicker red arrow than in a. We should note that similar considerations are valid for the case of an increased concentration of mobile ions.

These considerations are sufficient to formulate answers to the first two of our questions:

Illumination leads to an increase of the conductivity of the mobile ions. Therefore, it takes less time under reverse bias until the accumulation of mobile ions at the interface is significant. This accumulation leads to a larger reverse bias current.

We can translate that explanation to a fast voltage sweep: when the voltage sweep crosses a minimum reverse bias threshold, the mobile ions begin to move towards the

interfaces. While they are moving, the sweep continues and the reverse bias increases and accelerates them further. At some time Δt, the mobile ions reach the interface and reverse bias current begins to flow. The voltage that is applied at this time Δt appears as the breakdown voltage. A higher mobility (*e.g.* due to illumination) means that the mobile ions are faster. As they are faster, they reach the interface earlier, *i.e.* Δt is smaller. As Δt is smaller, the observed breakdown voltage appears smaller.

In the same way, an increased concentration means that, after the same Δt, a larger number of mobile ions has reached the interface. This means that a significant J_{RB} begins flowing earlier which again appears as a smaller V_{BD}.

The same argumentation also holds for the dependence of ΔV_{BD} on the scan rate:

We observed that under illumination ΔV_{BD} increases with smaller scan rate (see Fig. 3). This observation complies with our argumentation because the smaller scan rates give the mobile ions more time to react to the applied bias, *i.e.* "reach the interface". Δt is the same as before, but the voltage sweep is slower. That means that the voltage sweep has not progressed as far when the mobile ions reach the interface. That appears as a smaller breakdown voltage. Since the impact of scan rate on the dark V_{BD} is nearly negligible, the difference between dark and light V_{BD} increases and therefore ΔV_{BD} increases as well.

Finally, the illumination intensity was also observed to play a role. At low intensities, ΔV_{BD} increases steeply, but at higher intensities, the increase levels off (see Fig. 3). That means that additional photons have less of an effect at already higher illumination intensities (higher being here $\approx$0.05 suns). The same observation was made for CIGS solar cells.[26] There, they connected this illumination intensity-dependence to the excess charge carrier density. The same might be true for PSCs, as the interaction between mobile ions and light likely works *via* photo-generated charge carriers in the absorber.[40]

Thus, we successfully formulated explanations for our observations during fast voltage sweeps. They are based on the illumination affecting mobile ions and the accumulation of mobile ions at the interface affecting the breakdown voltage. The voltage scan rate affects the breakdown voltage only indirectly by determining which voltage is applied when enough mobile ions have arrived at the interfaces and have triggered the reverse bias breakdown. Instead, time (Δt) seems to be the decisive parameter.

However, our hypothesis in its current state does not explain the fundamentally different results at small scan rates (0.1 V s^{-1}). We would expect even smaller breakdown voltages than when we are using higher scan rates. Instead, we observe the pre-breakdown phenomenon, but barely any effect of illumination on the breakdown voltage. Therefore, we need to add an additional component to our hypothesis.

Like the reverse bias breakdown mechanism, this one was originally put forward in the publication of Bowring *et al.*[16] They observed an increase of the breakdown voltage over time while applying a constant reverse bias and proposed an electrochemical reaction at an interface as explanation.[16] This electrochemical reaction is expected to enhance the tunneling barrier and consequently increase the breakdown voltage, or decrease the reverse bias current. We follow one of the authors' proposals in regards to the mechanism and will assume in the following that this electrochemical reaction is the neutralization of mobile ions by charge carriers that constitute the reverse bias current. For the sake of comprehensibility, we will call them neutralized mobile "ions", even though they are, of course, not ions anymore after being neutralized. Neutralized mobile ions do not cause band bending which means that the electrochemical reaction leads to the tunneling barrier increasing in width. This reduces the probability of tunneling and decreases the reverse bias current.

The reaction rate of an electrochemical reaction is proportional to the current I.[41] That means for our case, that the number of neutralized mobile ions N_{neut} at a time Δt is determined by the charge Q that has flowed through the device until Δt:

$$N_{neut} \propto \int_{t=0}^{\Delta t} I\,dt = \int_{t=0}^{\Delta t} \frac{Q}{t}\,dt \quad (1)$$

This is the point where the voltage scan rate comes into play: during a measurement with a smaller scan rate, it takes more time for the cell to reach V_{BD} and the cell operates in the reverse bias regime for longer (Δt is larger). Therefore, during this longer time, more charge is flowing through the cell and more mobile ions are neutralized. It follows that there are less mobile ions present at the interface and band bending is less pronounced. Thus, V_{BD} appears to be larger. In contrast, when using a higher scan rate, the time that the solar cell spends in reverse bias is shorter. Therefore, the effect of the electrochemical reaction is less strong and the V_{BD} appears to be smaller. Again, it is the time Δt that is the decisive parameter. The difference between a sweep with 1 V s^{-1} and 0.1 V s^{-1} regarding the charge flowing through the cell is shown in the SI Fig. 10.

With that in mind, we have found a mechanism that has the potential to counteract the effect of illumination on the reverse bias breakdown. One increases and one decreases the breakdown voltage. In reality, both mechanisms are interdependent and act in parallel. This is schematically displayed in Fig. 5.

There, a simplified PSC is depicted with transport layers (TL1, TL2) and the perovskite absorber PVK. Under illumination, photo-activated mobile ions are present with a high mobility. Under the influence of the reverse bias ($-V$), they drift towards an interface. After some time (Δt), the first mobile ions reach the interface and contribute to the reverse bias breakdown mechanism. A current (J_{RB}) starts to flow (red arrow).

This reverse bias current leads to the neutralization of some mobile ions. They turn into black-filled circles with a red edge. These do not affect the reverse bias breakdown anymore. Thus, this neutralization compensates for the additionally arriving mobile ions. As many mobile ions are neutralized as newly arrived at the interface. Therefore, the current does not increases (the a red arrow is as thin as before).

In a voltage sweep, the slowly increasing reverse bias increases the number of arriving mobile ions faster than they are neutralized. We observe a slow increase of the current.

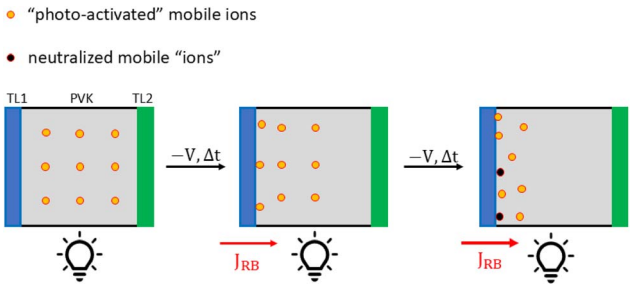

Fig. 5 A schematic representation of the two counteracting mechanisms: a simplified PSC is depicted with transport layers (TL1, TL2) and the absorber layer (PVK). Within the absorber, the photo-activated mobile ions are depicted as orange-filled circles with red edge. Under the reverse bias ($-V$) and in time (Δt), they move towards the interfaces. There, the mobile ions contribute to the breakdown mechanism and allow reverse bias current (J_{RB}) to flow (red arrow). However, the reverse bias current neutralizes some of the photo-generated mobile ions (they turn into black-filled circles with a red edge). After neutralization, they do not affect the reverse bias breakdown anymore. Therefore, this neutralization slows the increase of J_{RB} down.

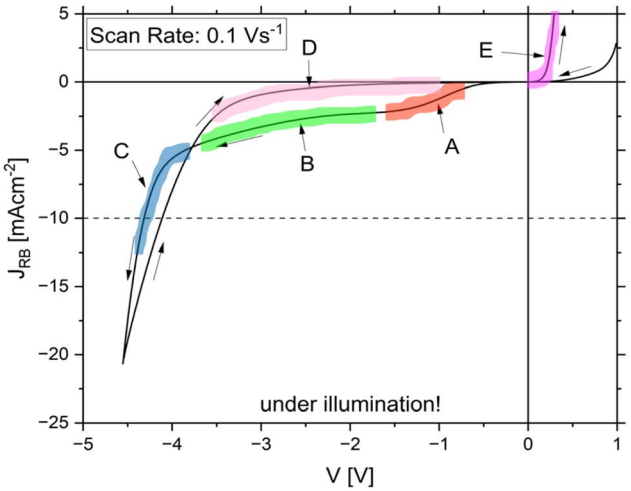

Fig. 6 A single light RB-*JV* curve after correction for the photo-generated current from a voltage sweep experiment with a scan rate of 0.1 V s^{-1}. Both RV and FW sweeps are shown. Five regions of interest are marked in color. (A) Shows the aborted early breakdown, (B) the period of near constancy of the current density, and (C) the actual reverse bias breakdown. (D) Highlights that the 'pre-breakdown' is not present in the FW sweep, and (E) shows the drastically changed behavior in the positive voltage region of the FW sweep.

Therefore, there must be a limiting factor to the neutralization reaction. That also explains why we observe the normal, exponential breakdown at a high reverse bias. At some point, it seems that the accumulation of mobile ions surpasses the neutralization reaction. Then, the near-balance between the two antagonistic mechanisms is broken.

3.2 Applying the hypothesis

This combined hypothesis, consisting now of two counteracting mechanisms, can explain our remaining observations concerning the light RB-*JV* measurements with a smaller scan rate (0.1 V s^{-1}). In the following, we will take a closer look at the RB-*JV* curve of such a measurement and apply our hypothesis to explain the relevant observations. This light RB-*JV* curve (corrected for the photo-generated current) is displayed in Fig. 6 where we have defined five different regions that we will discuss in more detail:

Region A (marked in red) contains the pre-breakdown that is only present in the RV sweep. Until this point ($V \approx -1$ V), only the first component of our hypothesis (the standard reverse bias breakdown mechanism including the effect of illumination) is playing a role. An early breakdown like in the RB-*JV* curves with high scan rates begins to appear. Here, the reverse bias current starts to increase, *i.e.* charge carriers are flowing. They exert their influence *via* the second component of our hypothesis (the electrochemical reaction) and partially counteract the effect of the reverse bias: a part of the mobile ions arriving at the interface is neutralized and therefore does not contribute to the band bending. The early exponential breakdown is aborted.

In region B (marked in green), a near-balance between the two antagonistic mechanisms is established. It seems that the increase of the voltage barely has an additional impact on the number of mobile ions at the interface. Most of the newly arriving mobile ions are neutralized, so that the reverse bias current increases only slightly.

In region C (marked in blue), the exponential breakdown finally occurs. It seems that the breakdown mechanism gains supremacy over the inhibiting mechanism at a similar voltage as in the dark. A possible reason for this change could be that illumination activates a second species of mobile ions with a higher mobility than the (original) species that is present in the dark. Then, the onset of region C would mark the voltage where the original ion species begins to play the dominant role in the reverse bias breakdown again.

Region D (marked in pink) highlights the low-current density regime of the FW sweep where the 'pre-breakdown' behavior is not visible. In this part of the measurement, the reverse bias is slowly decreasing. That means that the driving force behind the reverse bias breakdown diminishes. However, as long as the cell is still operating in reverse bias and there is still reverse bias current flowing, there is no impetus for turning the neutralized mobile ions back into their original states (*e.g.* reducing them). Thus, the state that leads to the pre-breakdown does not recur in the FW sweep. Instead, it looks very similar to the sweeps in the dark.

To formulate it in a simpler way: the RV sweep looks at the cell before and during a 'reverse bias current treatment' (the sweep itself). The reverse bias current during this 'treatment' increases V_{BD}. The FW sweep, on the other hand, looks at the cell after the application of this 'reverse bias current treatment', when the V_{BD} has already been increased. Thus, the 'pre-breakdown phenomenon' is not present.

Finally, region E (marked in violet) shows the behavior of the cell in the positive voltage region in the FW sweep. It might be interpreted as a discharge of charge that has been stored in the cell. This might be connected to the re-ionization of previously neutralized mobile ions.

Thus, we have demonstrated that our hypothesis can explain the observed phenomena. In order to strengthen our case, however, we have performed additional experiments designed to test the hypothesis. They will be presented in the following section.

4 Testing the hypothesis

We have developed a hypothesis and applied it to explain the previously described phenomena. It is based on two antagonistic mechanisms: firstly, illumination affects the conductivity of mobile ions. These mobile ions play a decisive role in the reverse bias breakdown. Secondly, the charge flowing through the solar cell in reverse bias leads to a increase of V_{BD} and therefore limits the RB current. The scan rate is involved by determining the time that mobile ions have to react to the voltage. Additionally, the scan rate also determines how long the solar cell remains in reverse bias and through that, how much charge flows through it. The time (Δt) is a core element of our hypothesis.

4.1 Experiment 1: the effect of illumination in (quasi-) steady state

In order to test our hypothesis, we have designed an experiment that allows us to investigate the effect of illumination on the reverse bias behavior outside of voltage sweeps. In that way, the effect of time, independent of voltage scan rate, should be more obvious. The experimental procedure is schematically displayed in Fig. 7. We inject a fixed current density J_{inj} into the solar cell in the dark and measure the voltage $V(t)$. We wait until the voltage has stabilized and the cell has reached a quasi-steady state. Then, we add illumination with a blue LED. According to our previous results, the wavelength of the illumination does not have a significant impact. We show that this is also true for the (quasi-) steady state experiment in the SI (Fig. 11). The illumination intensity is chosen such that $P_{light} \sim 0.1J_{inj}$. In that way, the solar cell continues to operate in a similar reverse bias regime as in the dark. We continue measuring the voltage with the light switched on.

We performed this experiment on various cells, using two different values for J_{inj}. A measurement with a current density of $J_{inj} = -10$ mA cm^{-2} allows the investigation of the breakdown voltage as this current density was used for defining V_{BD} in the voltage sweeps. The illumination intensity (following $P_{light} \sim 0.1J_{inj}$) corresponds to $P_{light} \approx 0.05$ in the RB-JV measurements. A representative voltage curve is displayed in Fig. 8a.

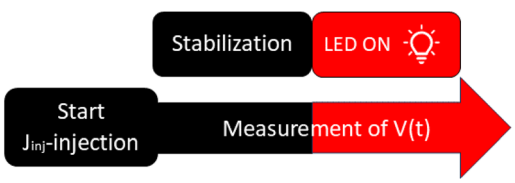

Fig. 7 A schematic representation of the experimental procedure of the quasi-steady state experiment. Here, a fixed current is injected while the voltage is measured. After a period of stabilization of the voltage in the dark, the LED is switched on.

The second value is $J_{inj} = -1$ mA cm^{-2}. Here the illumination intensity (following $P_{light} \sim 0.1J_{inj}$) is equivalent to $P_{light} \approx 0.005$. The idea behind this choice is that voltage and current density are smaller which should slow the processes driven by either of them. Additionally, it is the current density regime where the pre-breakdown phenomenon is visible in the voltage sweeps with a small scan rate. The results of this version of the quasi-steady state experiment are displayed in Fig. 8b.

We will first look at the results in Fig. 8a: there, the first observation is that the voltage increases in the first second and then decreases again over an initial period of 20 s. The voltage in the first few seconds is around -5 V, which fits the breakdown voltages observed during the voltage sweeps in the dark quite well. After 40 s, the voltage seems to stabilize at a slightly smaller voltage ($V \approx -4.3$ V). Here, we switched on the LED.

After the addition of illumination, we observe that the voltage decreases but only by $\Delta V \approx 0.05$ V. This decrease lasts for less than 1 ms (measurement period), then another process leads to an increase of the voltage by $\Delta V \approx 0.15$ V over a period of $t \approx 2$ s. Afterwards, other processes are taking over which are hard to distinguish from the processes generally occurring within the cells during reverse bias.

Focusing on the second version of this experiment in Fig. 8b with $J_{inj} = -1$ mA cm^{-2}, we observe the (quasi-)stabilization of the voltage after $t \approx 60$ s at a voltage of $V \approx -3.5$ V. Upon addition of illumination, the voltage decreases drastically to $V \approx -2$ V within $t \approx 5$ s. Over the following 70 s, the voltage slowly increases again until it reaches the voltage it showed before we added illumination.

The behavior of the solar cell in the first seconds in the dark is probably heavily influenced by the history of the solar cell and possibly by the sudden injection of a reverse bias current (capacitative effects). This undefined behavior was the reason for waiting for the voltage to stabilize before adding illumination. Therefore, discussing this effect in more detail is beyond the scope of this publication.

More interesting for us is the reaction to the addition of illumination: in Fig. 8a at $J_{inj} = -10$ mA cm^{-2}, we observe a very fast reaction in the form of a small voltage decrease and then a slower voltage increase. However, both voltage changes are barely significant if compared to the voltage applied as they amount to only a few percent. Therefore, it seems that the addition of illumination barely has an impact on V_{BD} at this current density level. At $J_{inj} = -1$ mA cm^{-2}, we observe the opposite: the voltage shifts significantly and then very slowly returns to the initial value. Do these results fit to the previous experiments?

If a voltage sweep is slow enough, the solar cells should reach a quasi-steady state in between the measurement points. Therefore, we will compare the results from the quasi-steady state experiment with the results from the voltage sweeps with a smallest employed scan rate 0.1 V s^{-1}.

There, we had observed only a very slight change of V_{BD} (see Fig. 3, black squares). That corresponds to a very slight change of the voltage at $J_{RB} = -10$ mA cm^{-2}. In the quasi-steady state

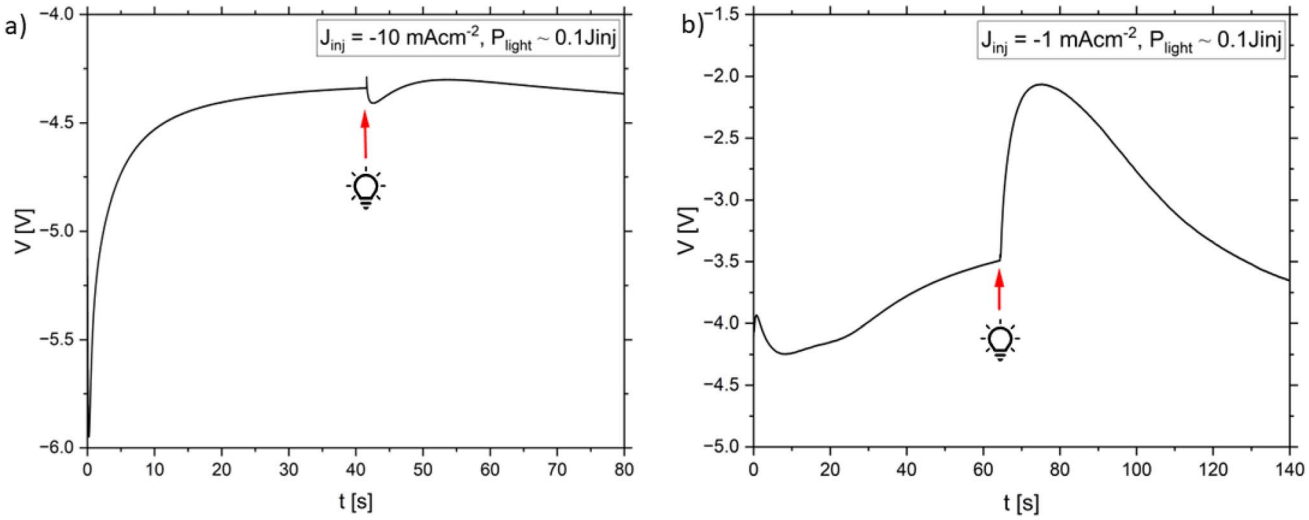

Fig. 8 Representative experimental results from the quasi-steady state-experiments with blue illumination: (a) shows the results for $J_{inj} = -10$ mA cm^{-2}. (b) Shows the results for $J_{inj} = -1$ mA cm^{-2}. In both cases, the red arrow and bulb symbol marks the time when the illumination is added.

experiment at $J_{RB} = -10$ mA cm^{-2}, we also have not seen a significant voltage shift upon addition of illumination (Fig. 8a). Thus, the results from slow voltage sweeps and from quasi-steady state measurement are in agreement in regards to the impact of illumination on V_{BD}.

In the low current density regime (≤ -3 mA cm^{-2}), we had observed the pre-breakdown behavior in the slow voltage sweeps (see Fig. 2c and 6). This phenomenon was only present in the RV sweep and not in the FW sweep. In the quasi-steady state experiment, we should see results equivalent to the RV and FW sweeps clearly separated in time. That is exactly what Fig. 8b shows: the initial decrease of the voltage upon addition of illumination corresponds to the pre-breakdown phenomenon. There, we observed a significant difference between dark and light RB-*JV* at this low current density level, too. With further flow of charge through the solar cell, this voltage decrease slowly vanishes and a state close to the dark is regained. That corresponds to the results of the FW sweep where we barely saw a difference between the dark and light RB-*JV* curves.

The same experiments using different cells showed qualitatively the same results. They are presented in the SI Fig. 12 and 13.

With these additional experiments, we have confirmed the important role that time is playing in the processes surrounding the interaction of illumination and reverse bias. In the low current density-regime, we have observed significant and slow changes to the voltage over timescales ranging from 1 s to 100 s. These findings do not only confirm our hypothesis of time being the decisive factor, but also support our explanation for the pre-breakdown phenomenon specifically: the difference between RV and FW sweep lies in the amount of charge that has flowed through the cell which is determined by the time the cell has spent in reverse bias. In the high current density-regime, we observed only insignificant changes to the voltage due to illumination, thus affirming the same observations regarding V_{BD} from the slow voltage sweeps.

4.2 Experiment 2: voltage sweeps after a pre-conditioning step

While the experiments in Section 4.1 already provide experimental support for our hypothesis, a more direct confirmation is desirable: so, we have performed a modified version of the previously presented voltage sweep experiment. The experimental procedure is displayed in Fig. 9a–c. It consists of a group of RB-*JV* measurements with a scan rate of 1 V s^{-1}. As before, eight measurements are performed in darkness and seven in various states of illumination. Dark and light *JV* measurements are alternated. However, this time, a pre-conditioning step before the first *JV* measurements is added to the procedure. We pre-condition the solar cell by injecting a current density of -10 mA cm^{-2} for 60 s in the dark. Additionally, we start and end the RB-*JV* measurements at $V = 0$ V in order to prevent recovery while the cell is forward biased.

The idea behind this experiment is the following: previously, we argued that the RB-*JV* measurements with a small scan rate (*e.g.* 0.1 V s^{-1}) do not show a significant impact of illumination on V_{BD} because a large amount of charge is flowing through the cell during the measurement and increases the tunneling barrier and with that V_{BD} (see Fig. 5). The same is not true for the *JV* measurements with a higher scan rate (*e.g.* 1 V s^{-1}), because the higher scan rate means a faster sweep and less time spent in reverse bias. Therefore, less charge flows through the cell and so, the effect of illumination that decreases V_{BD} dominates (see Fig. 4).

During this experiment, the pre-conditioning should bring the cell into a state where V_{BD} has already been increased. By avoiding positive biases during the voltage sweeps, we prevent the cell from recovering between the RB-*JV* measurements.

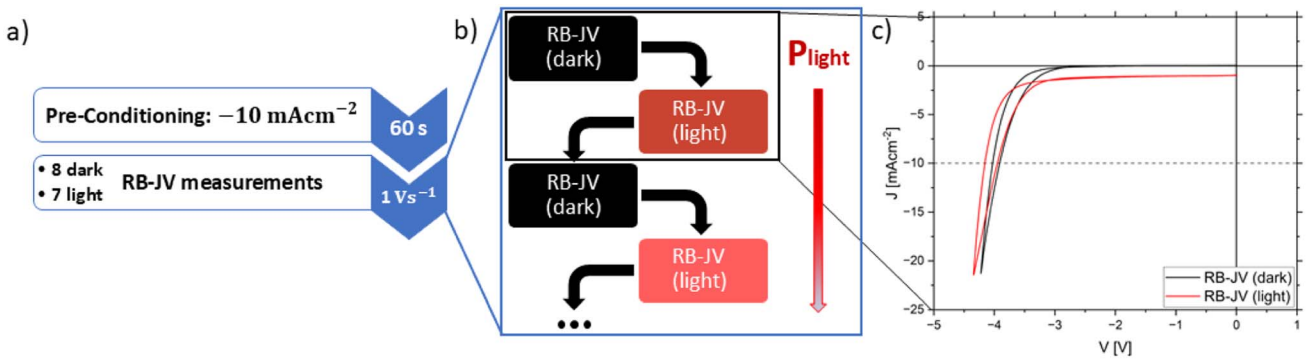

Fig. 9 The experimental procedure of the modified voltage sweep experiment. (a) After a pre-conditioning step, 15 RB-*JV* measurements are executed of which eight are dark and seven are light RB-*JV* measurements. They start and stop at $V = 0$ V. (b) Dark and light measurements are alternated and the illumination intensity increases from measurement to measurement. (c) We receive pairs of dark and light RB-*JV* curves.

Therefore, we expect to see a very limited impact of illumination on V_{BD} despite using a high voltage scan rate.

The measurement results are presented in Fig. 10.

In Fig. 10a, the RB-*JV* curves are shown. The dark RB-*JV* curves are plotted as black lines, the light RB-*JV* curves in shades of red. Both RV and FW sweeps are shown. We see that the black curves are nearly lying on top of each other as we had observed in previous experiments. This time, however, the red curves are also nearly inseparable. They are also shifted slightly to larger voltages in comparison with the black curves. These results bear a strong resemblance to the previous results from measurements with 0.1 V s^{-1} (compare Fig. 2b). In contrast to those, however, there is barely any difference between RV and FW sweep visible. In other words, the 'pre-breakdown' phenomenon is missing.

In Fig. 10b, the ΔV_{BD} calculated from RV and from FW sweeps are plotted against the illumination intensity. For comparison, results from a previous experiment without pre-conditioning are added to the graph. For the case with pre-conditioning, we see that $\Delta V_{BD} \approx 0$ V for all illumination intensities. Again, a strong resemblance to the previous results with a small scan rate of 0.1 V s^{-1} is observed. The contrast to the measurement results with the same scan rate but without pre-conditioning (in light green triangles) is striking.

These results show that the behavior of our PSCs during voltage sweeps is indeed influenced by the reverse bias current before or during the measurement. That supports our hypothesis that the main difference between small and high scan rates lies in the amount of charge that flows through the solar cell. The absence of a pre-breakdown after pre-conditioning fits to our explanation of this phenomenon, too: we explained it with the electrochemical reaction occurring during the voltage sweep and increasing V_{BD}. Here, that process has already occurred during the pre-conditioning and is therefore not visible in the voltage sweep. Therefore, we speculate that a pre-conditioning or an equivalent history of the solar cells could be a reason for the lack

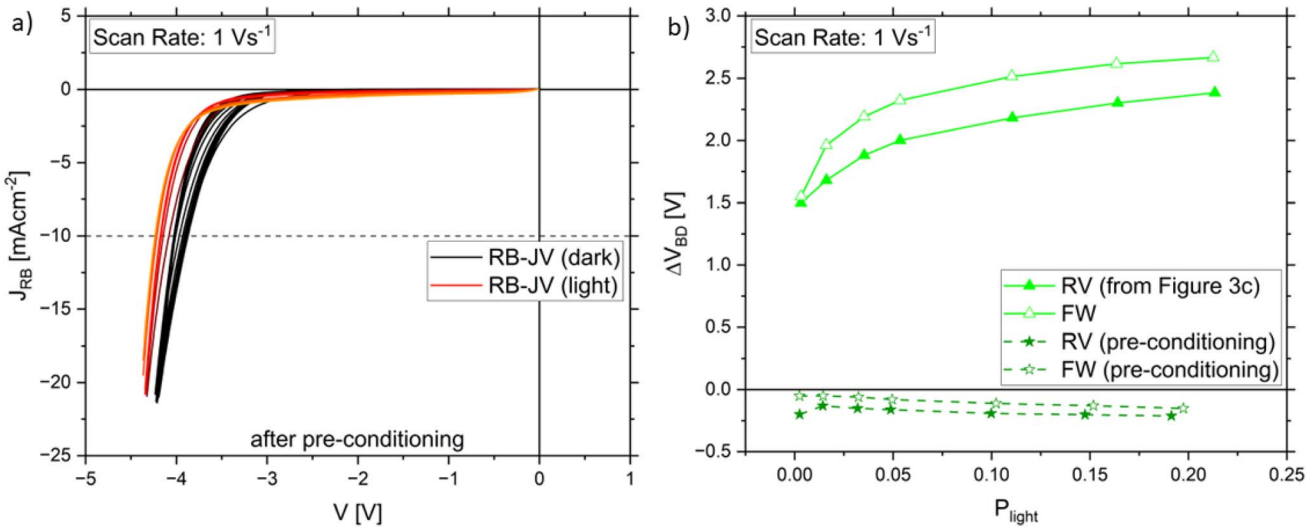

Fig. 10 Results of the modified voltage sweep experiment using a blue LED: (a) shows the RB-*JV* curves (RV and FW sweeps) with a scan rate of 1 V s^{-1} after pre-conditioning the cell. The black curves correspond to measurements in the dark, the red curves to light measurements. (b) Shows ΔV_{BD} against the illumination intensity determined from the curves in (a) and for a case without pre-conditioning for comparison.

of the pre-breakdown phenomenon in the RB-*JV* curves with illumination in Jiang *et al.*[25] However, this could also be explained by possible differences in ion mobility or concentration.

With that, we have shown two additional experiments that corroborate our hypothesis. As both the migration of mobile ions and the electrochemical reactions in the reverse bias regime are likely general, intrinsic phenomena that are not restricted to specific perovskite formulations or device designs, it should be also valid for different PSCs than the ones investigated in this study. Especially the results of *JV* measurements, however, depend strongly on the concentration or mobility of the mobile ions. These properties can vary strongly with the perovskite formulation employed and even the details of fabrication. Therefore, the scan rates necessary to observe the phenomena described in this study and time scales on which they occur, might differ. Additionally, the transport layers also seem to play an important role in the reverse bias breakdown mechanism and as a likely place for the electrochemical reaction to occur. Therefore, variations in transport layer material and device architecture might not modify the impact of illumination directly but the V_{BD} in the dark and the electrochemical reaction. Finally, there are open questions regarding the electrochemical reaction and the limiting factors to it. Investigating them in more detail was beyond the scope of this publication and was relegated to a future study.

5 Conclusions

The lack of stability against partial shading-induced degradation is one of the hurdles that the perovskite PV technology needs to overcome before commercialization. Solving this issue will require research effort on module and on cell level. One of the key details of the latter is the reverse bias breakdown. However, despite its importance, the mechanism of the reverse bias breakdown and its interplay with important perovskite solar cell properties (*e.g.* ion conductivity) or external factors (*e.g.* illumination, temperature) have still not been investigated in detail. Additionally, there are not even generally-agreed upon measurement procedures in place, and how the breakdown voltage is determined and defined in literature varies wildly.

In this publication, we observed that the reverse bias behavior under low-intensity illumination shows a strong dependence on the voltage scan rate. To explain this new phenomenon, we developed and tested a hypothesis based on two antagonistic mechanisms: on one hand, illumination increases the ion conductivity (mobility and/or concentration) which leads to smaller breakdown voltages than in the dark. On the other hand, an electrochemical reaction driven by the reverse bias current leads to an increase of the breakdown voltage. The scan rate determines how long the solar cell spends under reverse bias conditions and therefore how much time the mechanisms have to take effect. While the first mechanism is dominant in fast voltage scans, the second mechanism supersedes it at small voltage scan rates.

Our findings emphasize that more basic research on the behavior of perovskite solar cells in reverse bias is required: even well-known effects (*i.e.* of illumination on mobile ions conductivity) can lead to surprising results when combined with the rarely-regarded conditions in the reverse bias regime. While the hysteresis phenomenon and its dependence on the voltage scan rate has attracted much interest in the research community, the equivalent phenomenon in reverse bias has not yet been investigated in detail at all and is in most publications on the reverse bias behavior not even reported. And despite the temperature coefficient of the breakdown voltage being one of the decisive properties distinguishing avalanche from tunneling breakdown, a detailed investigation of the temperature-dependence of the V_{bd} in perovskite solar cells is still missing. Furthermore, without a basic understanding of the parameters influencing the voltage sweeps in reverse bias (*e.g.* scan rate), it is difficult to define test conditions and procedures that lead to comparable breakdown voltage values across different perovskite solar cells.

Investigating these fundamental relationships is necessary to understand the mechanisms underlying the reverse bias behavior of perovskite solar cells. However, additional to research on cells, actual partial shading investigations on perovskite modules should be intensified. We expect that the different sizes of cells in modules and the scribes play a role in the partial shading stability as well. Only with such a thorough understanding, we will be able to integrate highly stable cell technology with intelligent module design to achieve the partial shading stability that is necessary for the commercialization of the perovskite PV technology.

Author contributions

Jonathan Henzel: methodology, formal analysis, resources, investigation, writing – original draft, visualization Klaas Bakker: methodology, resources, writing – review & editing Sjoerd Veenstra: project administration, writing – review & editing Olindo Isabella: supervision, writing – review & editing Luana Mazzarella: supervision, writing – review & editing Arthur Weeber: supervision, writing – review & editing Mirjam Theelen: funding acquisition, supervision, writing – review & editing, project administration.

Conflicts of interest

There are no conflicts to declare.

Data availability

Data for this article are available at 4TU.ResearchData at **https://doi.org/10.4121/c1b5dd37-a34f-498a-8800-e785cd6e004a.v2**.

The SI contains the details about the fabrication of the samples, the results of the initial characterization, and detailed information about the other experiments. Furthermore, it includes additional experimental data that supports the conclusions drawn in the article. See DOI: **https://doi.org/10.1039/d5ta04100g**.

Acknowledgements

We acknowledge Johannes Lambooij and Corné Frijters for their part in the fabrication of samples. This work is funded through governmental funding *via* the Kennis Investerings Project (KIP) Solar and the Early Research Program (ERP) STAR of TNO financed by the Ministry of Climate Policy and Green Growth and Ministry of Economic Affairs.

References

1 M. Green, E. Dunlop, M. Yoshita, N. Kopidakis, K. Bothe, G. Siefer, X. Hao and J. Jiang, *Prog. Photovoltaics Res. Appl.*, 2024, 3–15.
2 P.-H. Hsi and J. C. P. Shieh, *Sustainability*, 2024, **16**, 3880.
3 M. Grätzel, *Nat. Mater.*, 2014, **13**, 838–842.
4 M. Khenkin, H. Köbler, M. Remec, R. Roy, U. Erdil, J. Li, N. Phung, G. Adwan, G. Paramasivam, Q. Emery, E. Unger, R. Schlatmann, C. Ulbrich and A. Abate, *Energy Environ Sci.*, 2023, **17**, 602–610.
5 M. V. Khenkin, E. A. Katz, A. Abate, G. Bardizza, J. J. Berry, C. Brabec, F. Brunetti, V. Bulović, Q. Burlingame, A. Di Carlo, R. Cheacharoen, Y. B. Cheng, A. Colsmann, S. Cros, K. Domanski, M. Dusza, C. J. Fell, S. R. Forrest, Y. Galagan, D. Di Girolamo, M. Grätzel, A. Hagfeldt, E. von Hauff, H. Hoppe, J. Kettle, H. Köbler, M. S. Leite, S. F. Liu, Y. L. Loo, J. M. Luther, C. Q. Ma, M. Madsen, M. Manceau, M. Matheron, M. McGehee, R. Meitzner, M. K. Nazeeruddin, A. F. Nogueira, C. Odabaşı, A. Osherov, N. G. Park, M. O. Reese, F. De Rossi, M. Saliba, U. S. Schubert, H. J. Snaith, S. D. Stranks, W. Tress, P. A. Troshin, V. Turkovic, S. Veenstra, I. Visoly-Fisher, A. Walsh, T. Watson, H. Xie, R. Yıldırım, S. M. Zakeeruddin, K. Zhu and M. Lira-Cantu, *Nat. Energy*, 2020, **5**, 35–49.
6 D. Lan and M. A. Green, *Joule*, 2022, **6**, 1782–1797.
7 S. Dongaonkar, C. Deline and M. A. Alam, *IEEE J. Photovoltaics*, 2013, **3**, 1367–1375.
8 E. J. Wolf, I. E. Gould, L. B. Bliss, J. J. Berry and M. D. McGehee, *Sol. RRL*, 2021, **6**, 2100239.
9 D. Bogachuk, K. Saddedine, D. Martineau, S. Narbey, A. Verma, P. Gebhardt, J. P. Herterich, N. Glissmann, S. Zouhair, J. Markert, I. E. Gould, M. D. McGehee, U. Würfel, A. Hinsch and L. Wagner, *Sol. RRL*, 2021, **6**, 2100527.
10 Y. Yang, C. Liu, Y. Ding, B. Ding, J. Xu, A. Liu, J. Yu, L. Grater, H. Zhu, S. S. Hadke, V. K. Sangwan, A. S. R. Bati, X. Hu, J. Li, S. M. Park, M. C. Hersam, B. Chen, M. K. Nazeeruddin, M. G. Kanatzidis and E. H. Sargent, *Nat. Energy*, 2024, 316–323.
11 T. Tayagaki, H. Kobayashi, K. Yamamoto, T. N. Murakami and M. Yoshita, *Sol. Energy Mater. Sol. Cells*, 2025, **279**, 113229.
12 R. Aninat, K. Bakker, J. Henzel, V. Zardetto, I. Dogan, V. Gevaerts, S. Veenstra and M. Theelen, *Prog. Photovoltaics Res. Appl.*, 2025, 1–9.
13 K. Bakker, A. Weeber and M. Theelen, *J. Mater. Res.*, 2019, **34**, 3977–3987.
14 T. J. Silverman, M. G. Deceglie, X. Sun, R. L. Garris, M. A. Alam, C. Deline and S. Kurtz, *2015 IEEE 42nd Photovoltaic Specialist Conference*, PVSC 2015, 2015, vol. 5, pp. 1742–1747.
15 R. A. Z. Razera, D. A. Jacobs, F. Fu, P. Fiala, M. Dussouillez, F. Sahli, T. C. J. Yang, L. Ding, A. Walter, A. F. Feil, H. I. Boudinov, S. Nicolay, C. Ballif and Q. Jeangros, *J. Mater. Chem. A*, 2020, **8**, 242–250.
16 A. R. Bowring, L. Bertoluzzi, B. C. O'Regan and M. D. McGehee, *Adv. Energy Mater.*, 2018, **8**, 1702365.
17 C. Wang, L. Huang, Y. Zhou, Y. Guo, K. Liang, T. Wang, X. Liu, J. Zhang, Z. Hu and Y. Zhu, *Adv. Energy Mater.*, 2023, **13**, 2203596.
18 J. Henzel, K. Bakker, M. Najafi, V. Zardetto, S. Veenstra, O. Isabella, L. Mazzarella, A. Weeber and M. Theelen, *ACS Appl. Energy Mater.*, 2023, **6**, 11429–11432.
19 L. J. Geerligs, M. Najafi, N. J. Bakker, D. Zhang, A. J. Carr, N. J. J. Dekker, J. Luiken, G. Coletti and S. C. Veenstra, *TandemPV Workshop*, 2022.
20 Y. Ma, Y. Cheng, X. Xu, M. Li, C. Zhang, S. H. Cheung, Z. Zeng, D. Shen, Y. Xie, K. L. Chiu, F. Lin, S. K. So, C. Lee and S. Tsang, *Adv. Funct. Mater.*, 2021, **31**, 2006802.
21 Z. Ni, H. Jiao, C. Fei, H. Gu, S. Xu, Z. Yu, G. Yang, Y. Deng, Q. Jiang, Y. Liu, Y. Yan and J. Huang, *Nat. Energy*, 2021, **7**, 65–73.
22 X. Guo, N. Li, Y. Xu, J. Zhao, F. Cui, Y. Chen, X. Du, Q. Song, G. Zhang, X. Cheng, X. Tao and Z. Chen, *Adv. Funct. Mater.*, 2023, 2213995.
23 J. Wang, G. Nie, W. Huang, Y. Guo, Y. Li, Z. Yang, Y. Chen, K. Ding, Y. Yang, W. Wang, L.-M. Kuang, K. Yang, D. Tang and Y. Zhai, *Nano Lett.*, 2024, **24**, 11873–11881.
24 N. Li, Z. Shi, C. Fei, H. Jiao, M. Li, H. Gu, S. P. Harvey, Y. Dong, M. C. Beard and J. Huang, *Nat. Energy*, 2024, **9**, 1264–1274.
25 F. Jiang, Y. Shi, T. R. Rana, D. Morales, I. E. Gould, D. P. McCarthy, J. A. Smith, M. G. Christoforo, M. Y. Yaman, F. Mandani, T. Terlier, H. Contreras, S. Barlow, A. D. Mohite, H. J. Snaith, S. R. Marder, J. D. MacKenzie, M. D. McGehee and D. S. Ginger, *Nat. Energy*, 2024, **9**, 1275–1284.
26 S. Puttnins, S. Jander, A. Wehrmann, G. Benndorf, M. Stölzel, A. Müller, H. V. Wenckstern, F. Daume, A. Rahm and M. Grundmann, *Sol. Energy Mater. Sol. Cells*, 2014, **120**, 506–511.
27 P. Szaniawski, J. Lindahl, T. Törndahl, U. Zimmermann and M. Edoff, *Thin Solid Films*, 2013, **535**, 326–330.
28 C. Wang, L. Huang, Y. Guo, S. Liu, J. Huang, X. Liu, J. Zhang, Z. Hu, K. Liu and Y. Zhu, *Sol. RRL*, 2023, **7**, 1–11.
29 V. M. Le Corre, J. Diekmann, F. Peña-Camargo, J. Thiesbrummel, N. Tokmoldin, E. Gutierrez-Partida, K. P. Peters, L. Perdigón-Toro, M. H. Futscher, F. Lang, J. Warby, H. J. Snaith, D. Neher and M. Stolterfoht, *Sol. RRL*, 2022, **6**, 2100772.

30 Y. Shao, Y. Fang, T. Li, Q. Wang, Q. Dong, Y. Deng, Y. Yuan, H. Wei, M. Wang, A. Gruverman, J. Shield and J. Huang, *Energy Environ Sci.*, 2016, **9**, 1752–1759.
31 J. S. Yun, J. Seidel, J. Kim, A. M. Soufiani, S. Huang, J. Lau, N. J. Jeon, S. I. Seok, M. A. Green and A. Ho-Baillie, *Adv. Energy Mater.*, 2016, **6**, 1–8.
32 W. Li, K. Huang, J. Chang, C. Hu, C. Long, H. Zhang, X. Maldague, B. Liu, J. Meng, Y. Duan and J. Yang, *ChemPhysMater*, 2022, **1**, 71–76.
33 D. A. Jacobs, C. M. Wolff, X.-Y. Chin, K. Artuk, C. Ballif and Q. Jeangros, *Energy Environ. Sci.*, 2022, **15**, 5324–5339.
34 M. Auf der Maur, F. Matteocci, A. Di Carlo and M. Testa, *Appl. Phys. Lett.*, 2022, **120**, 113505.
35 H. J. Snaith, A. Abate, J. M. Ball, G. E. Eperon, T. Leijtens, N. K. Noel, S. D. Stranks, J. T.-W. Wang, K. Wojciechowski and W. Zhang, *J. Phys. Chem. Lett.*, 2014, **5**, 1511–1515.
36 D. A. Jacobs, Y. Wu, H. Shen, C. Barugkin, F. J. Beck, T. P. White, K. Weber and K. R. Catchpole, *Phys. Chem. Chem. Phys.*, 2017, **19**, 3094–3103.
37 E. J. Juarez-Perez, R. S. Sanchez, L. Badia, G. Garcia-Belmonte, Y. S. Kang, I. Mora-Sero and J. Bisquert, *J. Phys. Chem. Lett.*, 2014, **5**, 2390–2394.
38 J. Xing, Q. Wang, Q. Dong, Y. Yuan, Y. Fang and J. Huang, *Phys. Chem. Chem. Phys.*, 2016, **18**, 30484–30490.
39 Y. Zhao, W. Zhou, Z. Han, D. Yu and Q. Zhao, *Phys. Chem. Chem. Phys.*, 2021, **23**, 94–106.
40 A. Schiller, S. Jenatsch, B. Blülle, M. A. Torre Cachafeiro, F. Ebadi, N. Kabir, M. Othman, C. M. Wolff, A. Hessler-Wyser, C. Ballif, W. Tress and B. Ruhstaller, *J. Phys. Chem. Lett.*, 2024, 11252–11258.
41 M. Faraday, *Philos. Trans. R. Soc. London*, 1834, **124**, 77–122.